

# Spatio-temporal dynamics of $\beta$ -tubulin isotypes during the development of the sensory auditory organ in rat

Justine Renauld<sup>1</sup> · Nicolas Johnen<sup>1</sup> · Nicolas Thelen<sup>1</sup> · Marie Cloes<sup>1</sup> · Marc Thiry<sup>1</sup>

Accepted: 5 June 2015  
© Springer-Verlag Berlin Heidelberg 2015

**Abstract** There are different  $\beta$ -tubulin isoforms in microtubules of vertebrate tissues. However, their functional significance is still largely unknown. In the present study, we investigated the localization of five  $\beta$ -tubulin isotypes ( $\beta$ 1–5) within the hearing organ during development in rat. By using confocal microscopy, we showed that with the exception of the  $\beta$ 3-tubulin isoform that was specific to nerve fibres, all the different  $\beta$ -tubulin isoforms were mainly present in the supporting cells. Contrary to  $\beta$ 1–4-tubulins, we also found that the  $\beta$ 5-tubulin isoform appeared only at a key stage of the post-natal development in specific cell types (pillar cells and Deiters' cells). By using transmission electron microscopy, we revealed further that this developmental stage coincided with the formation of two separate bundles of microtubules from a unique one in these supporting cells. Together, these results suggest that the  $\beta$ 5-tubulin isoform might be involved in the generation of new microtubule bundles from a pre-existing one.

**Keywords** Microtubules · Development · Confocal microscopy · Transmission electron microscopy

Justine Renauld and Nicolas Johnen have contributed equally to this article.

**Electronic supplementary material** The online version of this article (doi:10.1007/s00418-015-1350-2) contains supplementary material, which is available to authorized users.

✉ Justine Renauld  
justine.renauld@ulg.ac.be

✉ Marc Thiry  
mthiry@ulg.ac.be

<sup>1</sup> Unit of Cell and Tissue Biology, GIGA-Neurosciences, University of Liege, CHU Sart-Tilman, B36, 4000 Liege, Belgium

## Introduction

Microtubules constitute one of the major components of the cytoskeleton in eukaryotic cells and are involved in many essential processes, including cell division and ciliary and flagellar motility (Etienne-Manneville 2013; Lee and Norden 2013; Akhshi et al. 2014). They are also essential for cell migration and axon development, and are required, along with actin filaments and intermediate filaments, for the dynamic spatial organization of the cytoplasm (Joshi et al. 1985; Tischfield et al. 2010).

Microtubules are long, hollow cylinders of approximately 25 nm in diameter made up of the association of protofilaments that are aligned parallel to the long axis of the tubule. A protofilament is formed by tubulin heterodimers associated in a head-to-tail manner. Heterodimers consist of  $\alpha$ - and  $\beta$ -tubulin isotypes, each encoded by distinct genes. Seven isotypes of mammalian  $\beta$ -tubulin have been characterized, termed  $\beta$ 1,  $\beta$ 2,  $\beta$ 3,  $\beta$ 4a,  $\beta$ 4b,  $\beta$ 5 and  $\beta$ 6 (Ludueña 1998). With the exception of  $\beta$ 6, the  $\beta$ -tubulin isotypes are among the most highly conserved proteins known (Ludueña 1998).

The strict conservation of isotype-specific amino acid sequences over extensive periods of evolutionary time argues in favour of different functional roles for the different isotypes (Cowan et al. 1988). But the reason why vertebrates express seven different  $\beta$ -tubulin genes is not well understood (Yang et al. 2009).

Recently, some researchers (Hari et al. 2003; Bhattacharya and Cabral 2004; Bhattacharya et al. 2011; Yang et al. 2009) have shown that modulating the expression of some isotypes caused abnormalities in cell growth and altered sensitivity to drugs targeting microtubules.

Although the functional significance of the diversity of the  $\beta$ -tubulin is still unknown (Wade 2009), in 1976,

Fulton and Simpson suggested that the various isoforms of  $\beta$ -tubulin could mediate the different functional roles of microtubules (Fulton and Simpson 1976). As per this hypothesis, the isoforms would be selectively expressed in different tissues and may even be compartmentalized within cells according to their function (Perry et al. 2003). Consistently, it was found that different isoforms were expressed in different cell types of the same tissue (Lewis et al. 1985; Roach et al. 1998; Hallworth and Ludueña 2000). Moreover, it was demonstrated in invertebrates that the small amino acid sequence differences between  $\beta$ -tubulin isoforms were conserved for functional reasons. Genetically modified *Drosophila* testis expressing more than 6 % of a moth  $\beta$ -tubulin isoform exhibited the 16-protofilament structure characteristic of the moth on the corresponding subset of *Drosophila* microtubules, which normally contain only 13-protofilament microtubules (Raff 1997). Another example was the nematode worm *Caenorhabditis. elegans* in which all somatic cells have microtubules with 11 protofilaments except mechanosensory neurons of touch possessing microtubules with 15 protofilaments. This structural organization could be lost by the inhibition of *mec-12* ( $\alpha$ -tubulin) and *mec-7* ( $\beta$ -tubulin). The mutational studies indicated clearly that this specific heterodimer was essential in the formation of 15-protofilament microtubules and that this structure was fundamental for the touch sense (Savage et al. 1989; Fukushige et al. 1999; Bounoutas et al. 2009; Wade 2009).

The importance of the different  $\beta$ -tubulin isoforms was less well established in vertebrates. Nevertheless, Saillour and his collaborators (Saillour et al. 2014) revealed recently that the deletion of  $\beta$ 3-tubulin led to some developmental abnormalities in the brain that could not be rescued by any other  $\beta$ -tubulin isoforms. This observation supports the notion that even if they share significant homology and similar functions, each tubulin isoform may have a specific role (Saillour et al. 2014).

The organ of Corti, located within the cochlea, a portion of the inner ear, appears to be an excellent model for studying the role of  $\beta$ -tubulin isoforms. This epithelium is responsible for the transduction of sound waves into nerve impulses and is composed of two cellular types: the sensory cells and the non-sensory supporting cells (Fritzsche et al. 2014). This highly specialized epithelium contains different kinds of supporting cells: the phalangeal cell, the inner and outer pillar cells and Deiters' cells. Pillar and Deiters' cells are characterized by an abundant and highly ordered cytoskeleton framework (Henderson et al. 1995). Moreover, we already know that this tissue contains a particular type of microtubules. In fact, the organ of Corti is the only vertebrate tissue exhibiting microtubules with 15 protofilaments instead of the canonical 13 (Tucker et al. 1992). All these reasons support the choice of the organ of Corti to study the  $\beta$ -tubulin isoforms.

In the present work, we studied the spatio-temporal dynamics of each  $\beta$ -tubulin isoform during the development of the organ of Corti. Jensen-Smith and colleagues (2003) proposed that  $\beta$ -tubulin isoform compositions in the hair cells and pillar cells are the same at birth, before undergoing a selective reduction at late stages in post-natal development (Jensen-Smith et al. 2003). Unlike them, we showed that only some isoforms labelled these cells at early stages. Thus, we revealed for the first time that  $\beta$ 5-tubulin, a tubulin solely detected in adult gerbil cochlea (Banerjee et al. 2008), labelled specific cell types during key stages of the development of the organ of Corti.

## Materials and methods

### Animals

Animal handling was carried out in compliance with the University of Liege Animal Care and Use Committee guidelines that are in accordance with the Declaration of Helsinki. The Wistar rats were bred in our animal facility. The day of coitus was recorded as day 0 (E0), and the day of birth was recorded as post-natal day 0 (P0). Wistar rats were killed from E18 to P25. Seventy-three rats were killed for the immunolabellings (five at E18, five at E20, five at P0, five at P2, six at P4, six at P6, six at P8, five at P10, four at P12, four at P14, five at P16, four at P18, six at P20 and seven at P25) and six for the ultrastructural analyses (four at P4 and two at P25). Watchmaker forceps were used to dissect the cochleae under a stereomicroscope. The cochlear apex was carefully pierced to allow rapid penetration of the fixative.

### Immunohistochemistry

The cochleae were prepared as previously described (Cloes et al. 2013). They were fixed at 4 °C in a solution composed of 2 % formaldehyde in 0.1 M Sørensen's buffer pH 7.4 for 1 h. After several washes at 4 °C in Sørensen's buffer, the cochleae were decalcified at 4 °C in 4 % (w/v) EDTA in Sørensen's buffer as long as necessary. After that, the samples were washed several times in Sørensen's buffer and incubated at 4 °C in 30 % (w/v) sucrose in Sørensen's buffer on a gently rotating platform until full impregnation for cryopreservation. The cochleae were embedded in 7.5 % (w/v) gelatin 15 % (w/v) sucrose in Sørensen's buffer for 15 min at 37 °C. The preparation was finally plunged into an isopentane bath on dry ice for solidification. The cryosections (14  $\mu$ m thick) were obtained by means of a cryostat (Microm HM 560, Prosan).

The cryosections were rinsed in PBS (140 mM NaCl, 2.7 mM KCl, 1.5 mM  $\text{KH}_2\text{PO}_4$ , 16 mM  $\text{Na}_2\text{HPO}_4$ , pH

7.4) and permeabilized at room temperature in 1 % Triton X-100 PBS for 10 min. After several washes in PBS, the sections were blocked for 30 min at 37 °C with 10 % (v/v) normal goat serum (NGS) in PBS or 10 % NGS-1 % BSA in PBS. Then, the sections were incubated with the primary antibody solution diluted in 5 % NGS-PBS for 30 min at 37 °C or overnight at 4 °C, washed in PBS and incubated for 30 min at 37 °C with the secondary antibody diluted in PBS. After being washed in PBS, the nuclei were stained by incubating the sections with DAPI (1:50,000, 4',6-diamidino-2-phenylindole dihydrochloride, Sigma, St Louis, USA) at 37 °C for 15 min. Finally, the cryosections were rinsed in PBS and mounted with Citifluor AF1 (Laborimpex, Brussels, Belgium).

Primary antibodies were diluted in PBS containing 5 % of NGS at the following concentrations: rabbit anti-myosin VI polyclonal antibody (pAb) M5187 (1:150; Sigma, St Louis, USA), mouse anti- $\beta$ 1-tubulin monoclonal antibody (mAb) T7816 (1:100, Sigma, St Louis, USA), mouse anti- $\beta$ 2-tubulin monoclonal antibody (mAb) T8453 (1:100, Sigma, St Louis, USA), mouse anti- $\beta$ 3-tubulin monoclonal antibody (mAb) T5076 (1:100, Sigma, St Louis, USA), mouse anti- $\beta$ 4-tubulin monoclonal antibody (mAb) T7941 (1:100, Sigma, St Louis, USA), mouse anti- $\beta$ 5-tubulin monoclonal antibody (mAb) [1:100, gift from Dr Richard F. Ludueña (Department of Biochemistry, University of Texas Health Science Center at San Antonio, San Antonio, Texas)]. The secondary antibodies used were: goat anti-mouse Alexa 488 and goat anti-rabbit Alexa 594 (1:250, Molecular Probes, Leiden, The Netherlands). As a negative control, the primary antibody was omitted. In each case, no labelling was observed.

The mid- and basal turns of the cochlea were taken into consideration. The immunolabellings were examined under an Olympus IX71 confocal microscope. Acquisitions were made by using a  $\times$ 60 objective. The optical sections were analysed with the software FV10-ASW 1.7 Viewer.

### Electron microscopy

The cochleae were prepared as previously described (Thelen et al. 2009). They were fixed for 2 h at room temperature in 2.5 % glutaraldehyde in 0.1 M Sørensen's buffer pH 7.4. After several washes in the same buffer, the samples were post-fixed for 60 min with 2 % osmium tetroxide in Sørensen's buffer, washed in deionized water, dehydrated at room temperature through a graded ethanol series (70, 96 and 100 %) and embedded in Epon for 48 h at 60 °C. Ultrathin sections (70 nm thick) were obtained by means of an ultramicrotome (Reichert Ultracut E) equipped with a diamond knife (Diatome), were mounted on copper grids coated with collodion and were contrasted with uranyl acetate and lead citrate for 15 min each.

The basal turn of the cochlea was taken into consideration. Ultrathin sections were examined under a Jeol JEM-1400 transmission electron microscope at 80 kV and photographed with a 11 MegaPixel bottom-mounted TEM camera system (Quemesa, Olympus). The images were analysed via iTEM software.

## Results

To determine the precise localization of each  $\beta$ -tubulin isotypes during development of the Corti organ, we performed immunofluorescent labellings on cryosections of rat cochleae from E18 to P25 with specific antibodies against each of the five  $\beta$ -tubulin isotypes ( $\beta$ 1– $\beta$ 5). We also used as a benchmark myosin VI, a known marker of the sensory cells.

### $\beta$ 1-Tubulin isotype

At E20, we detected a weak labelling for  $\beta$ 1-tubulin in the phalangeal cells, in the basal parts of Deiters' cells and in the pillar cells (Fig. 1a). Until P25, no labelling occurred in the sensory cells (Fig. 1a–f). From P2, the fluorescent signal increased in the basal parts of Deiters' cells and in the apex of pillar cells (Fig. 1b). At P6 (Fig. 1c), the labelling became intense at these two locations. At P14, the phalangeal process of Deiters' cells contained  $\beta$ 1-tubulin isotype, but the immunostaining was weaker. From P14 until P25, pillar cells and Deiters' cells displayed an equal and thin labelling along the entire height of cells (Fig. 1d). At P16 (Fig. 1e), we observed the labelling of nerve fibre extensions reaching the outer hair cells (arrow) through the tunnel of Corti.

### $\beta$ 2-Tubulin isotype

During the embryonic stages, a  $\beta$ 2-tubulin isotype labelling was observed in the nerve processes (Fig. 2a), the apex of the inner hair cells and the outer hair cells, with a stronger signal for the third outer hair cells. At birth (Fig. 2b), we also detected an additional labelling in pillar cells and in the basal parts of Deiters' cell. At P6 (Fig. 2c), the labelling started to decrease in the sensory cells. At this stage, the labelling extended to the phalangeal process of Deiters' cells. From P10 to the adult stages (Fig. 2d–f), this isotype was strongly present in the pillar cells and Deiters' cells.

### $\beta$ 3-Tubulin isotype

This isotype is more restricted than the others in the organ of Corti. In fact,  $\beta$ 3-tubulin was only present in the nerve processes emanate from the spiral ganglion (Fig. 3a–f). As

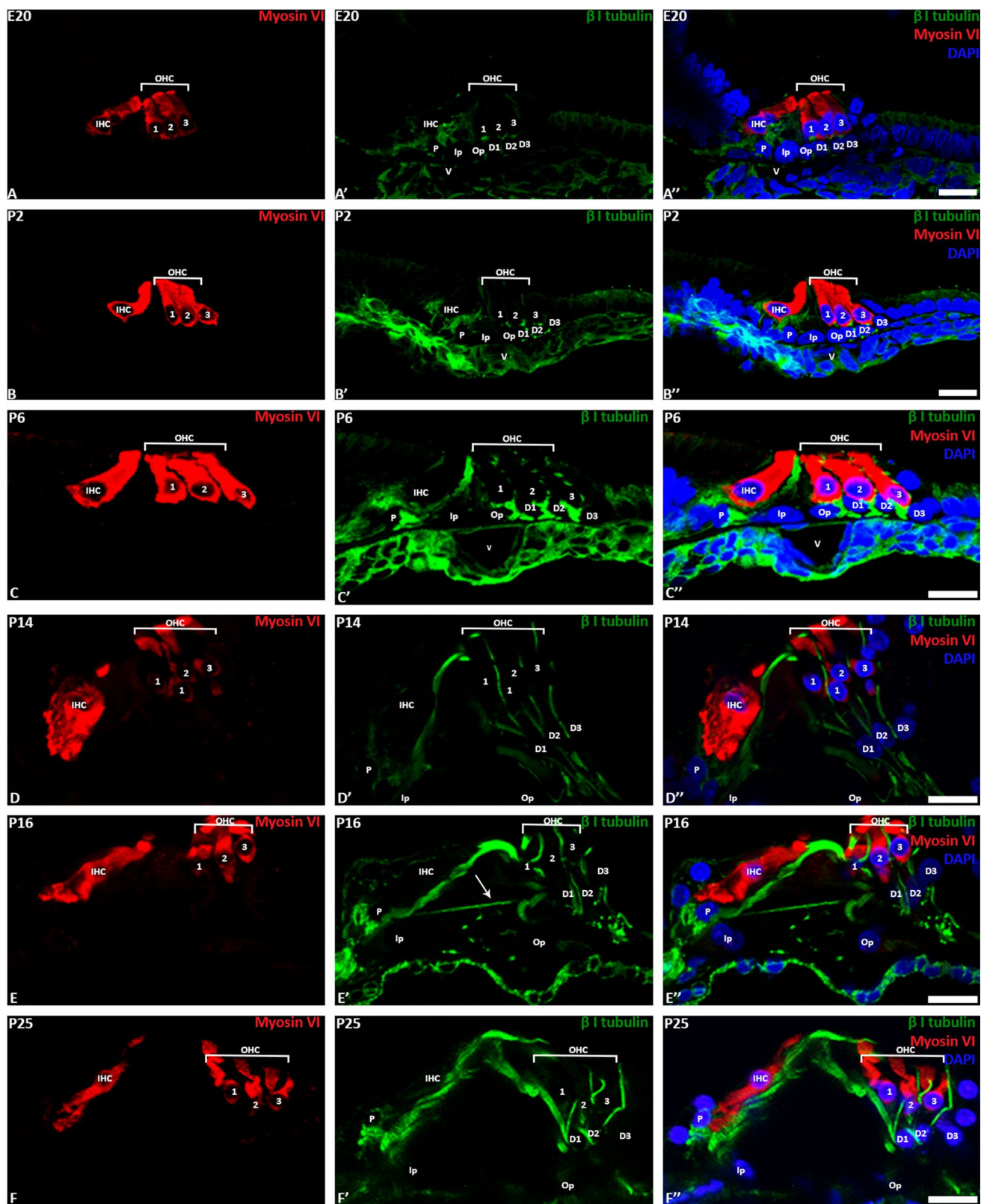


**Fig. 1** Immunolocalization of  $\beta 1$ -tubulin within the organ of Corti from E20 to P25. **a–f** Localization of the hair cells using myosin VI (red). **a'–f'** Immunolocalization of the  $\beta 1$ -tubulin (green). **a''–f''** Merged image with cell nuclei stained with DAPI (blue). **D(1–3)**

Deiters' cells, *Ip* inner pillar cell, *IHC* inner hair cell, *OHC(1–3)* outer hair cell, *Op* outer pillar cell, *P* phalangeal cell, *V* spiral vessel, *arrow* nerve process. Bar 20  $\mu\text{m}$

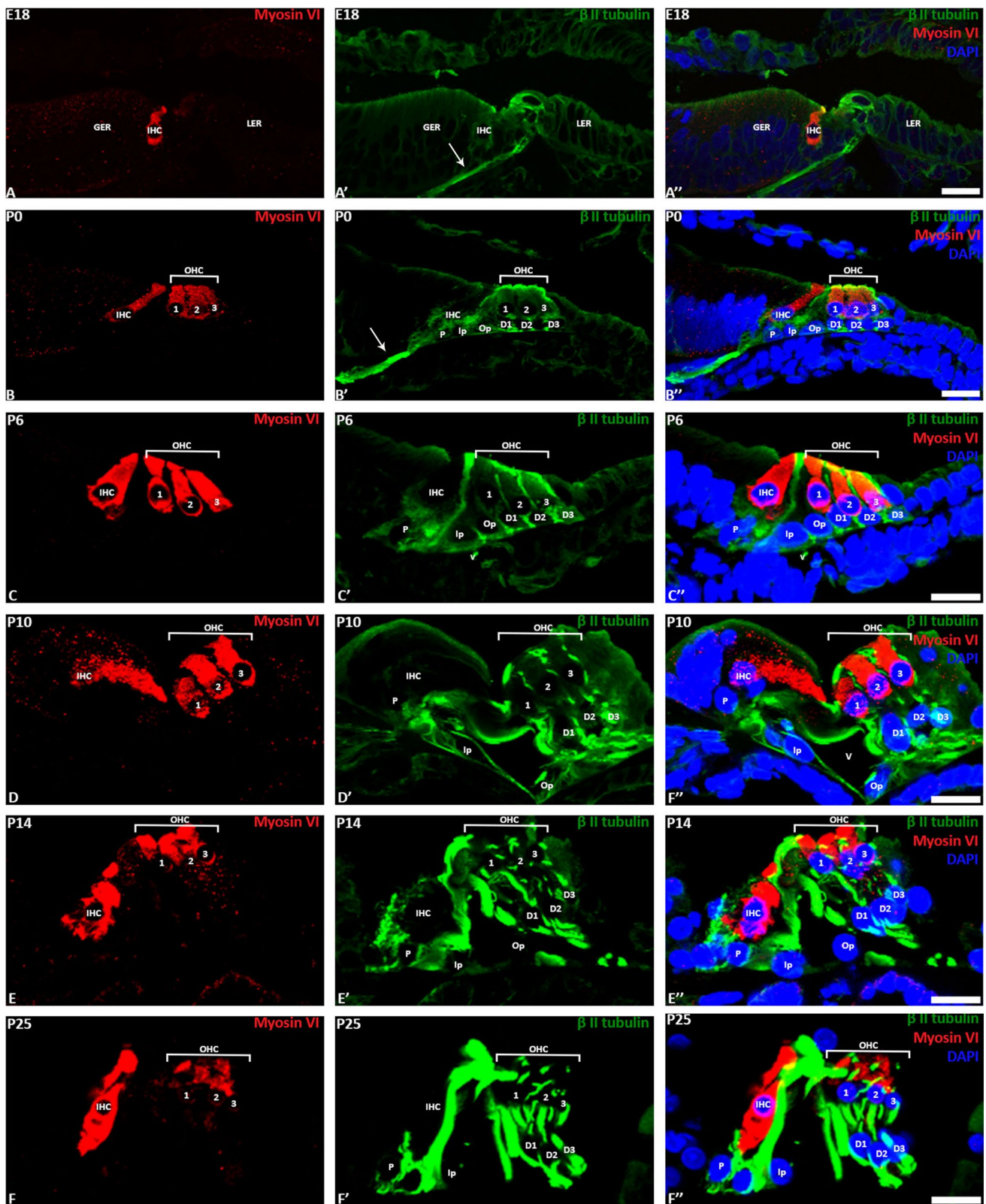


**Fig. 2** Immunolocalization of  $\beta 2$ -tubulin within the organ of Corti from E18 to P25. **a–f** Localization of the hair cells using myosin VI (red). **a'–f'** Immunolocalization of the  $\beta 2$ -tubulin (green). **a''–f''** Merged image with cell nuclei stained with DAPI (blue). *D(1–3)*

Deiters' cells, *Ip* inner pillar cell, *IHC* inner hair cell, *OHC(1–3)* outer hair cell, *Op* outer pillar cell, *P* phalangeal cell, *V* spiral vessel, *arrow* nerve process. *Bar* 20  $\mu\text{m}$

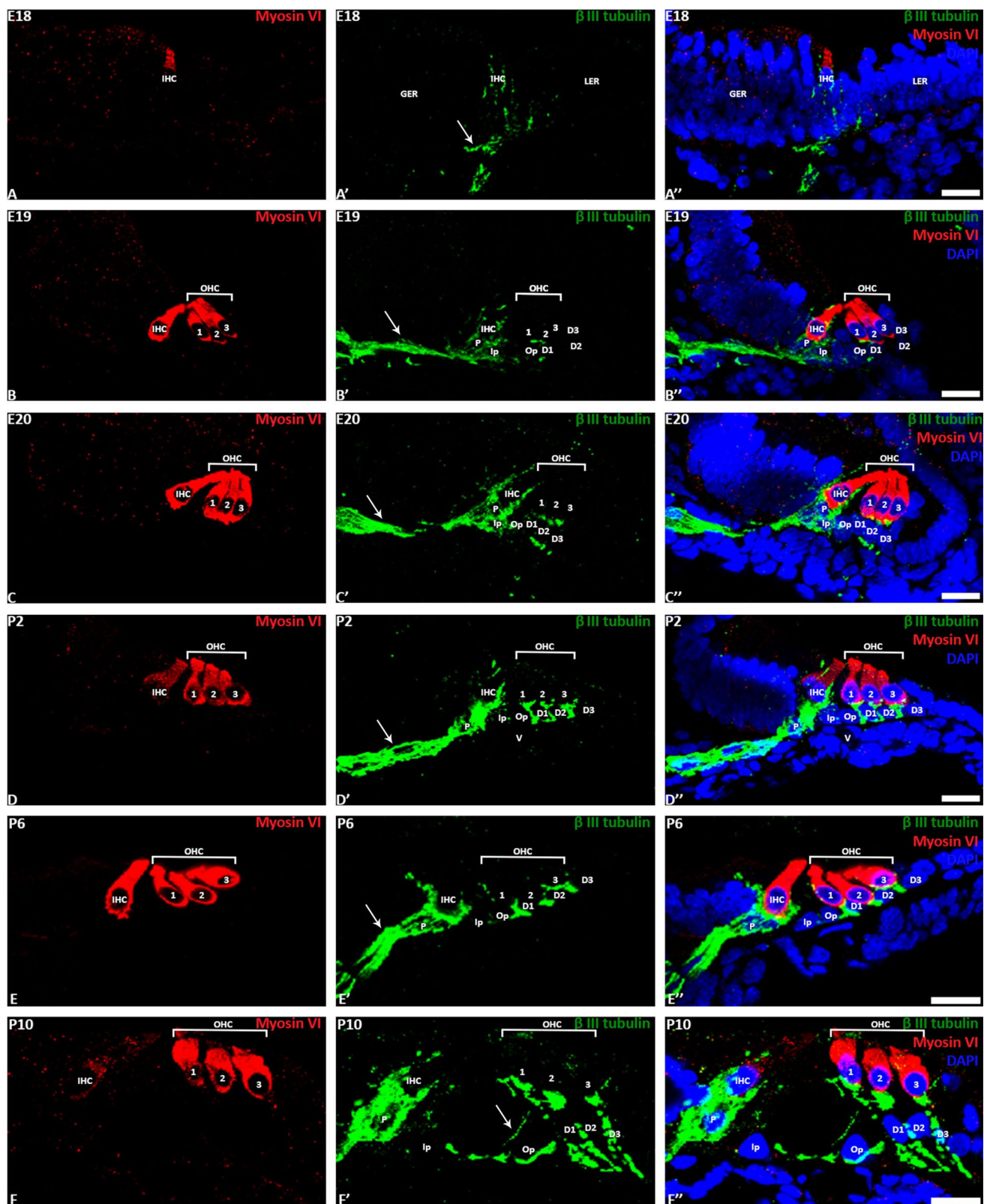


**Fig. 3** Immunolocalization of  $\beta 3$ -tubulin within the organ of Corti from E18 to P10. **a–f** Localization of the hair cells using myosin VI (red). **a'–f'** Immunolocalization of the  $\beta 3$ -tubulin (green). **a''–f''** Merged image with cell nuclei stained with DAPI (blue). *D(1–3)*

Deiters' cells, *Ip* inner pillar cell, *IHC* inner hair cell, *OHC(1–3)* outer hair cell, *Op* outer pillar cell, *P* phalangeal cell, *V* spiral vessel, *arrow* nerve process. *Bar* 20  $\mu\text{m}$

shown in Fig. 3, the  $\beta$ 3-tubulin was present at the embryonic stages (Fig. 3a–c). At E18 (Fig. 3a), a thin labelling was visible around the basal part of the inner hair cells. At E19 (Fig. 3b), the labelling extended to the basal part of the outer hair cells, with extensions stretched in the baso-lateral part of the inner hair cells. From P6 to the adult stage, the  $\beta$ 3-tubulin labelling was detected in the basal parts of each sensory cell, corresponding to the nerve fibres innervating the sensory cells. During the development of the organ of Corti, no labelling was found either in the sensory cells (inner hair cells and outer hair cells) or in the supporting cells (inner pillar cells, outer pillar cells, phalangeal cells and Deiters' cells).

### $\beta$ 4-Tubulin isotype

A  $\beta$ 4-tubulin labelling appeared at E20 in the inner hair cells (Fig. 4a). At this stage, the labelling was intense and spread in the entire height of these cells. At birth, the labelling of inner hair cells seemed to be less strong, and a signal appeared in the inner pillar cells (Fig. 4b). In pillar cells, the labelling is restricted to the apical part. At P4,  $\beta$ 4-tubulin was found in the entire height of the inner pillar cells (Fig. 4c). The signal in the inner hair cells was weak, like in the outer hair cells. At P8 (Fig. 4d), the immunolabelling was also detected in the outer pillar cells and Deiters' cells. P8 was the last developmental stage at which the sensory cells were  $\beta$ 4-tubulin-positive. From this stage, the signal for  $\beta$ 4-tubulin was intense in the supporting cells and remained until the adult stage.

### $\beta$ 5-Tubulin isotype

Unlike other  $\beta$ -tubulin isotypes, the  $\beta$ 5-tubulin was absent from the embryonic stages (Fig. 5a). This isotype appeared for the first time at P6 in the inner pillar cells (Fig. 5b). At P8 (Fig. 5c), the labelling was present in the inner pillar cells and weakly in the outer pillar cells and Deiters' cells. From P10 to the adult stage (Fig. 5d, e), a strong signal was found in the supporting cells (inner pillar cells, outer pillar cells and Deiters' cells), in particular in their basal parts and their phalangeal process.

### Transmission electron microscopy

To determine the precise localization of microtubules within the organ of Corti during development, we analysed rat cochleae at P4 and P25 using transmission electron microscopy.

#### *Deiters' cells*

At P4, the microtubules we observed were all oriented in the same direction, indicating the presence of a single microtubule bundle (arrowheads). However, they were less numerous

and less tight than those observed at P25 (Fig. 6a–c). They were parallel to the longitudinal axis of Deiters' cell. At the adult stage, Deiters' cells were clearly composed of two microtubule bundles (Fig. 6d–g). One bundle went through the phalangeal process of Deiters' cells (Fig. 6e). The other one went under the base of outer hair cells (Fig. 6f). Both bundles gathered together at the level of the cell nucleus and extended to the basilar membrane (Fig. 6g).

#### *Pillar cells*

At P4, we saw a single microtubule bundle starting from the apical part of the cell (Fig S9). In the adult stage, we clearly observed two bundles of microtubules perpendicular to each other (Fig S9 e, f).

## Discussion

This study is the first description of  $\beta$ -tubulin isotype distribution in the cochlear epithelium of the rat during the development of the organ of Corti from embryonic day E18 to post-natal day P25. Figure 7 shows the distribution of  $\beta$ -tubulin isoforms at two key developmental stages of the organ of Corti: the sixth post-natal day preceding the opening of the tunnel of Corti and the adult stage.

### Localization of $\beta$ -tubulin isotypes in the sensory cells and nerve processes

The first  $\beta$ -tubulin isotypes found during the development of the organ of Corti are the  $\beta$ 3-tubulin isotype and the  $\beta$ 2-tubulin isotype at E18. These two isotypes present a distinct localization: the  $\beta$ 3-tubulin is restricted to the nerve processes reaching the inner hair cells, while the  $\beta$ 2-tubulin spreads in the inner hair cells and outer hair cells of organ of Corti in addition to the nerve processes (Fig. 7; Table 1). One day later, the labelling of  $\beta$ 3-tubulin isotype appears in the nerve processes extending to the outer hair cells. At E20, the  $\beta$ 4-tubulin isotype shows an intense labelling in the inner hair cells. This labelling intensity decreases in inner hair cells at birth. These results reveal a difference in the localization of  $\beta$ 4-tubulin isotypes between the gerbil's organ of Corti and the rat's organ of Corti (Jensen-Smith et al. 2003). Moreover, the  $\beta$ 4-tubulin isotype was also detected in the outer hair cells of the adult gerbil's organ of Corti (Jensen-Smith et al. 2003), which was not the case in our study.

The immunolabelling of  $\beta$ 2-tubulin decreased with age and disappeared in the adult rat's sensory cells. Our results differ from those seen by other investigators (Steyger et al. 1989; Hallworth and Ludueña 2000; Jensen-Smith et al. 2003) as we did not observe any labelling of the sensory cells at the adult stages. This discrepancy could be due

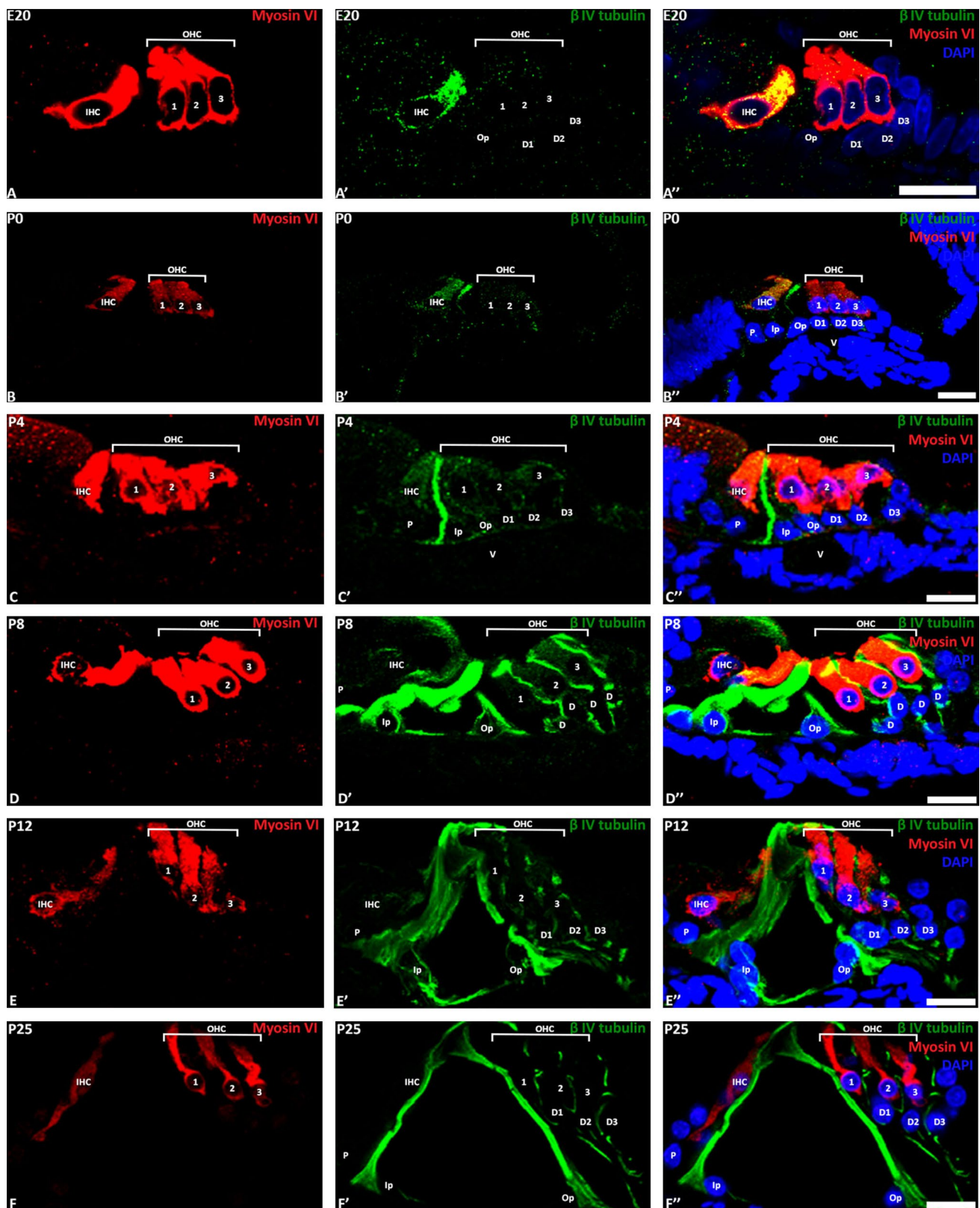


**Fig. 4** Immunolocalization of  $\beta$ 4-tubulin within the organ of Corti from E20 to P25. **a–f** Localization of the hair cells using myosin VI (red). **a'–f'** Immunolocalization of the  $\beta$ 4-tubulin (green). **a''–f''** Merged image with cell nuclei stained with DAPI (blue). *D(1–3)*

Deiters' cells, *Ip* inner pillar cell, *IHC* inner hair cell, *OHC(1–3)* outer hair cell, *Op* outer pillar cell, *P* phalangeal cell, *V* spiral vessel. Bar 20  $\mu$ m



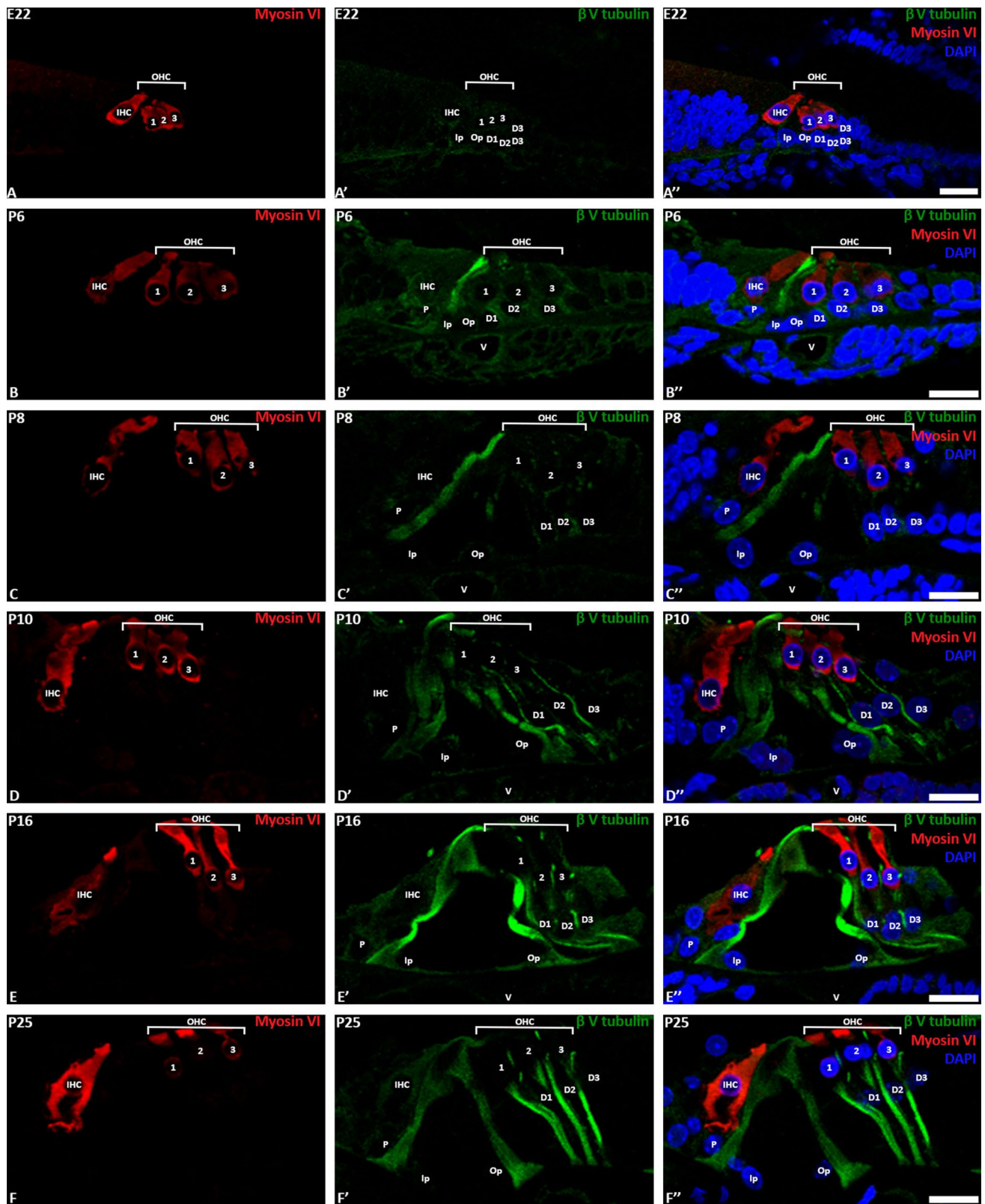
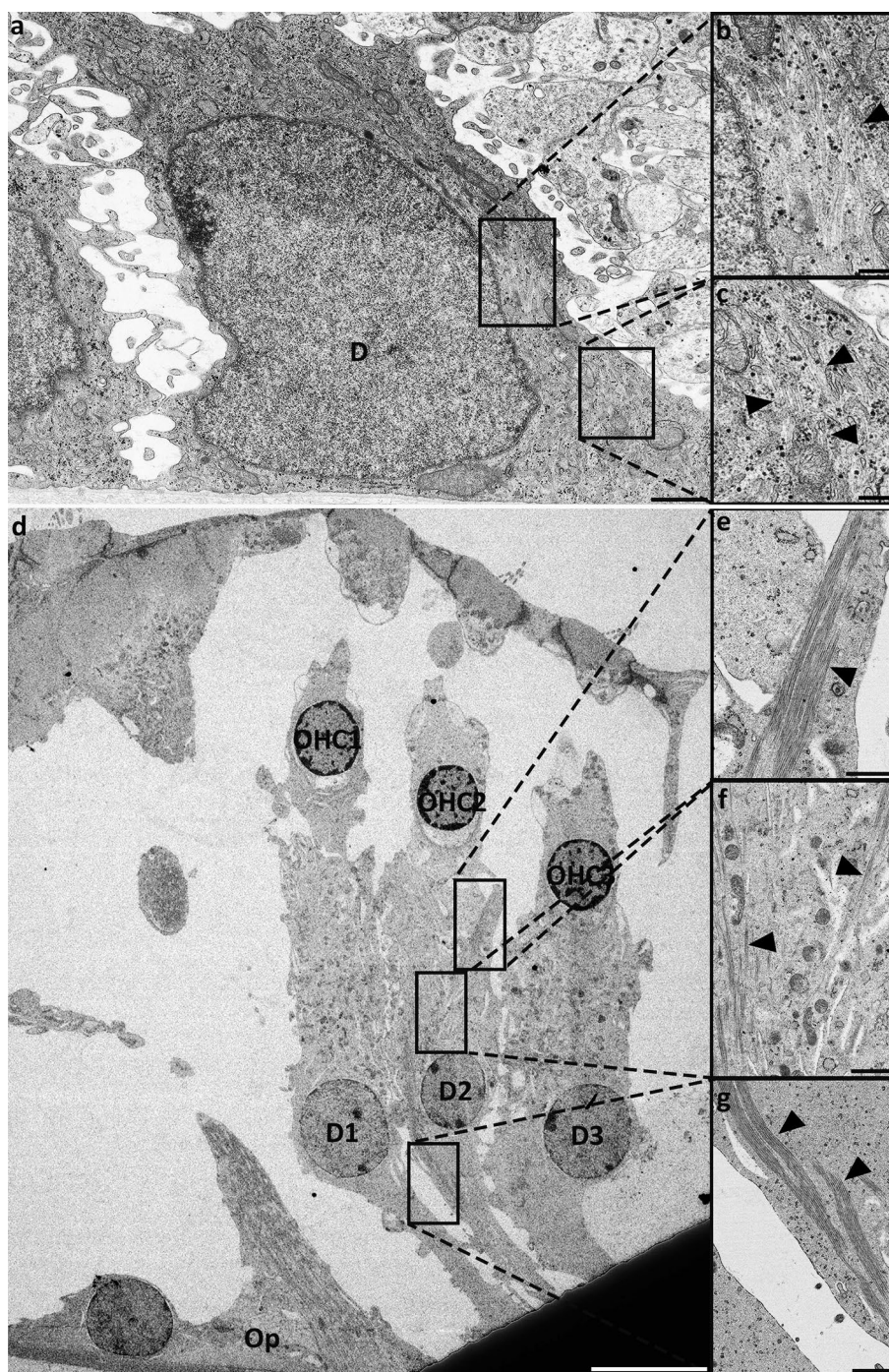


**Fig. 5** Immunolocalization of  $\beta 5$ -tubulin within the organ of Corti from E22 to P25. **a–f** Localization of the hair cells using myosin VI (red). **a'–f'** Immunolocalization of the  $\beta 5$ -tubulin (green). **a''–f''** Merged image with cell nuclei stained with DAPI (blue). *D(1–3)*

Deiters' cells, *Ip* inner pillar cell, *IHC* inner hair cell, *OHC(1–3)* outer hair cell, *Op* outer pillar cell, *P* phalangeal cell, *V* spiral vessel. Bar 20  $\mu$ m

**Fig. 6** Ultrastructure of Deiters' cells at P4 (**a–c**) and P25 (**d–g**). **a** General view. *Bar* 1  $\mu\text{m}$ . **b**, **c** Details of their cytoplasm containing microtubules (*arrowheads*). *Bar* 250 nm. **d** General view. *Bar* 10  $\mu\text{m}$ . **e** A microtubule bundle of the phalangeal process at high magnification. **f** An enlargement of the two microtubule bundles present in Deiters' cells (*arrowheads*). **g** An enlargement of these two bundles gathered together at the height of the cell nucleus and descending to the basilar membrane (*arrowheads*), *D(1–3)* Deiters' cells, *OHC(1–3)* outer hair cell, *Op* outer pillar cell. *Bar* 250 nm



to the antibody used. In fact, we used an antibody targeting amino acids 437–445 at the C-terminal sequence of human  $\beta$ 2-tubulin (EEEEGEDEA), which corresponds to the sequence of  $\beta$ 2-tubulin in the rat. The antibody used in both previous papers targets the C-terminal sequence of the chicken  $\beta$ 2-tubulin (EGEEDEA). It is nevertheless interesting to note that our weak labelling in the sensory cells is in agreement with the small amount of microtubules observed in these cells under electron microscopy (data not shown).

### Localization of $\beta$ -tubulin isotypes in the supporting cells

#### *Pillar cells*

At E18, the  $\beta$ 2-tubulin isotype weakly labelled supporting cells. At E20, the  $\beta$ 1-tubulin isotype was present in all supporting cells of the organ of Corti, along the full length of pillar cells. This localization remained the

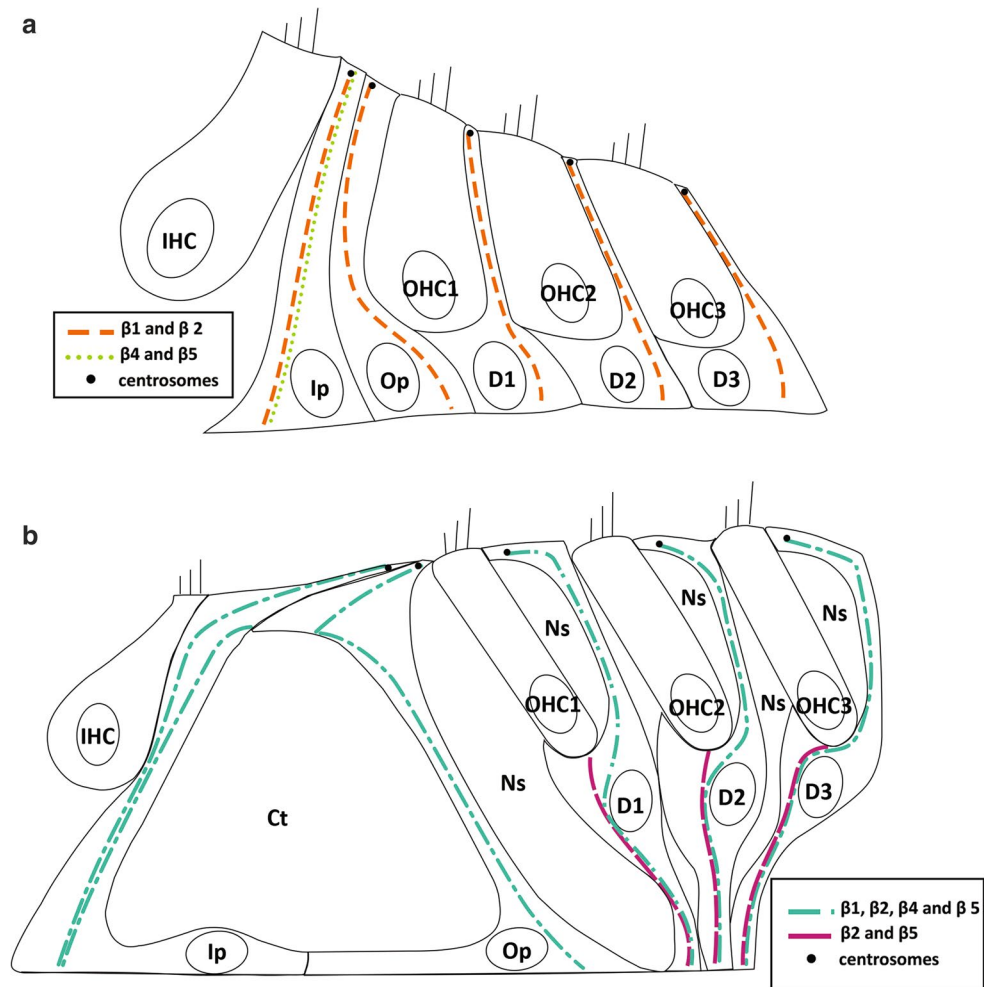


**Fig. 7** Schematic diagram of the organ of Corti showing the distribution of  $\beta$ -tubulin isotypes in the supporting cells at P6 (a) and P25 (b). *Ct* tunnel of Corti, *D* Deiters' cells, *Ip* inner pillar cell, *IHC* inner hair cell, *Ns* space of Nuel, *OHC* (1–3) outer hair cell, *Op* outer pillar

cell. Centrosomes are positioned according to data provided by Henderson, Tucker and their teams (Tucker et al. 1992, 1998; Henderson et al. 1994, 1995)

**Table 1** Localization of  $\beta$ -tubulin isotypes observed in each cell type of the organ of Corti during the development (E18–P25) in rat

	E18 → E22	P0	P2 → P4	P6	P8	P10 → P25
Nerves process	$\beta 2$ – $\beta 3$	$\beta 2$ – $\beta 3$	$\beta 3$	$\beta 3$	$\beta 3$	$\beta 3$
Inner hair cells	$\beta 2$ – $\beta 4$	$\beta 2$ – $\beta 4$	$\beta 2$ – $\beta 4$	$\beta 2$ – $\beta 4$	$\beta 2$ – $\beta 4$	
Outer hair cells	$\beta 2$	$\beta 2$	$\beta 2$ – $\beta 4$	$\beta 2$ – $\beta 4$	$\beta 4$	
Inner pillar cells	$\beta 1$	$\beta 1$ – $\beta 4$	$\beta 1$ – $\beta 4$	$\beta 1$ – $\beta 2$ – $\beta 4$ – $\beta 5$	$\beta 1$ – $\beta 2$ – $\beta 4$ – $\beta 5$	$\beta 1$ – $\beta 2$ – $\beta 4$ – $\beta 5$
Outer pillar cells	$\beta 1$	$\beta 1$	$\beta 1$	$\beta 1$ – $\beta 2$	$\beta 1$ – $\beta 2$ – $\beta 4$ – $\beta 5$	$\beta 1$ – $\beta 2$ – $\beta 4$ – $\beta 5$
Deiters' cells	$\beta 1$	$\beta 1$ – $\beta 2$	$\beta 1$ – $\beta 2$	$\beta 1$ – $\beta 2$	$\beta 1$ – $\beta 2$ – $\beta 4$ – $\beta 5$ / $\beta 2$ – $\beta 4$	$\beta 1$ – $\beta 2$ – $\beta 4$ – $\beta 5$ / $\beta 2$ – $\beta 4$

same at birth as at E20, which was in agreement with the results obtained in the gerbil (Jensen-Smith et al. 2003). Our results also showed the appearance, at birth, of this  $\beta 4$ -tubulin isotype in the upper part of the inner pillar cell. The labelling in the upper part of the pillar cell was consistent with the finding that inner pillar assembly begins

with the nucleation of a large microtubule population at the apical end of each cell (Tucker et al. 1992; Souter et al. 1997; Jensen-Smith et al. 2003). These results were also in agreement with our electron microscopy analysis of pillar cells at P4 (Fig S9). At P6,  $\beta 2$ -tubulin kept the same localization, while increasing the labelling in

the supporting cells. The  $\beta$ 4-tubulin was found along the entire height of the inner pillar cells.

At this stage, we saw for the first time the appearance of  $\beta$ 5-tubulin, another tubulin isotype never studied during the development of the organ of Corti until now (Fig. 7; Table 1). This tubulin appeared in the inner pillar cell and in the apex of the outer pillar cell. At P8, during the opening of the tunnel of Corti, the  $\beta$ 4 and  $\beta$ 5-tubulin isotypes extended their localization to the entire height of the outer pillar cell. From P8 to the adult stage,  $\beta$ 1-,  $\beta$ 2-,  $\beta$ 4- and  $\beta$ 5-tubulin isotypes were present in pillar cells (Fig. 7; Table 1).

#### *Deiters' cells*

At E18, the  $\beta$ 2-tubulin isotype weakly labelled the supporting cells. At E20, the  $\beta$ 1-tubulin isotype appeared in all the supporting cells of the organ of Corti, along with the basal part of Deiters' cells only, between the base of the outer hair cells and the basilar membrane. At birth, the labelling of this basal part of Deiters' cells was clearly visible with the  $\beta$ 2-tubulin isotype. At P6, these tubulin isotype labellings extended to the phalangeal process of Deiters' cells. At this stage, the basal part of Deiters' cells contained a wide band of  $\beta$ 1- and  $\beta$ 2-tubulin isotypes (Fig. 7; Table 1). At P8, just before the opening of the spaces of Nuel, the  $\beta$ 4- and  $\beta$ 5-tubulin isotypes extended their localization to Deiters' cells (Fig. 7; Table 1). From P8 to the adult stage, except  $\beta$ 3, all  $\beta$ -tubulin isoforms are present along the entire height of Deiters' cells with a wide band composed of  $\beta$ 2- and  $\beta$ 5-tubulin in the basal part (Fig. 7; Table 1).

In Fig. 3f, we observed a labelling for  $\beta$ 3-tubulin in the basal part of Deiters' cells, between the base of the outer hair cells and the reticular lamina.  $\beta$ 3-Tubulin is a well-known neuronal marker (Locher et al. 2013). This labelling can be related to nerve processes which cross the tunnel of Corti and reach the basal part of the outer hair cells, although we visualized some labelling under the nucleus of Deiters' cells. Some researchers had already shown the presence of nerve processes in the basal part of Deiters' cells (Parsa et al. 2012). They said that Deiters' cells showed, in their medial region, a distinctive envelopment of unmyelinated afferent nerves that were thought not to establish any synapse with them, so that our labelling could be explained by these afferent nerves.

Regarding the supporting cells, we clearly see that the localization of the different  $\beta$ -tubulins changes between P6 and P8 (Table 1). We have already shown that during this critical period, pillar and Deiters' cells undergo dramatic morphological and molecular changes (Johnen et al. 2012). It has also been demonstrated that during these stages, microtubules progressively develop to reach the large number found at the adult stage (Tucker et al. 1998; Hallworth

et al. 2000; Szarama et al. 2012). In the present paper, we report a huge increase in the labelling of pillar cells for all  $\beta$ -tubulin isotypes at P6, confirming these previous data. The most drastic change appeared in Deiters' cells, where the labelling increases in length and intensity. This labelling stretches out in the basal part due to the pull up of the cell nucleus. After the opening of the fluid spaces (i.e. the tunnel of Corti and the space of Nuel), the distribution of  $\beta$ -tubulin isotypes did not seem to progress as much as before. In the adult organ of Corti, we can easily conclude that  $\beta$ -tubulin isotypes are mostly present in the supporting cells. This result is in complete agreement with our electron microscopy data in which we show a large amount of microtubules in the supporting cells (Fig. 6).

Supporting cells undergo shape changes during post-natal development, after the differentiation of sensory cells. These shape changes allow the opening of the tunnel of Corti and spaces of Nuel, and appear before the establishment of hearing function. Several authors have shown the importance of intercellular spaces present within the organ of Corti (Karavitaki and Mountain 2007; Zagadou and Mountain 2012). They state that these fluid-filled spaces (tunnel of Corti and spaces of Nuel) facilitate the sound wave that supports OHC amplification. The establishment of microtubule bundles probably plays a significant role in maintaining this epithelial structure. Indeed, rigidity of these supporting cells must exist to allow the opening of such intercellular spaces without the collapse of the entire epithelium. The onset or upregulation of the expression of  $\beta$ -tubulin is probably related to the increase in microtubules present in these cells.

Using immunostaining, Slepecky and her collaborators (1995) suggested the presence of two different microtubule bundles in Deiters' cells: one spanning the distance between the base of the outer hair cells and the basilar membrane and another one between the base of the outer hair cells and reticular lamina (Slepecky et al. 1995). Here, our immunolabellings are consistent with the presence of two distinct microtubule bundles. A narrow one going from phalangeal processes to the nuclear region, labelled by  $\beta$ 1-,  $\beta$ 2-,  $\beta$ 4- and  $\beta$ 5-tubulin isotypes and a wide one going from the nucleus to the reticular lamina, labelled by the  $\beta$ 2- and  $\beta$ 5-tubulin isotypes. Our immunocytological results are in agreement with our electron microscopic observations. Indeed, we clearly visualized two microtubule bundles in Deiters' cells of an adult cochlea in longitudinal section. These results are consistent with the observations realized in gerbil (Henderson et al. 1995).

Another interesting result obtained in this study is the fact that the  $\beta$ 5-tubulin appeared in a key stage of the development of the organ of Corti. Contrary to the other  $\beta$ -tubulin isoforms, this isotype appears in pillar cells just before the opening of the tunnel of Corti, and in Deiters'

cells before the opening of Nuel's spaces. As shown with our electron microscopic analysis in the supporting cells, this period was characterized by the subdivision of one single microtubule bundle into two separated bundles. Furthermore, Tannenbaum and Slepecky (1997) has shown that these bundles formed by a large number of shorter microtubules (2000 out of the 3000 present in each inner pillar cell) are released from their apical anchoring site and migrate to the base of the cell, where their ends are captured at a basal anchoring site (Tannenbaum and Slepecky 1997).

Together, these data allow us to speculate that the  $\beta 5$ -tubulin isotype might be a particular  $\beta$ -tubulin involved in the detachment of microtubules from the bundle associated with the centrosome in pillar and Deiters' cells. In this context, it is interesting to remember that in cancerous cells, the overexpression of  $\beta 5$ -tubulin disrupts microtubule organization and induces microtubule detachment from the centrosome (Bhattacharya and Cabral 2004; Bhattacharya et al. 2011). If our suggestion proves correct, it will support the multi-tubulin hypothesis which states that each isotype of tubulin mediates the different functional roles of microtubules (Fulton and Simpson 1976; Wade 2009).

**Acknowledgments** We thank Mrs P. Piscicelli for her skilful technical assistance and Dr. Richard F. Ludueña (Department of Biochemistry, University of Texas Health Science Center at San Antonio, San Antonio, Texas) for generous gift of the antibody anti- $\beta 5$ -tubulin. We thank the GIGA-Imaging and Flow Cytometry platform for technical support. This work was supported by Fonds de la recherche scientifique (FNRS-FRS). J.R. and N.J. are PhD grant holders of the FRIA. M.C. was a FRS-FNRS Research Fellow.

#### Compliance with ethical standards

**Conflict of interest** The authors declare no conflict of interest.

## References

- Akhshi TK, Wernike D, Piekny A (2014) Microtubules and actin crosstalk in cell migration and division. *Cytoskeleton* 71:1–23. doi:10.1002/cm.21150
- Banerjee A, Jensen-Smith H, Lazzell A et al (2008) Localization of  $\beta$ v tubulin in the cochlea and cultured cells with a novel monoclonal antibody. *Cell Motil Cytoskeleton* 65:505–514. doi:10.1002/cm.20280
- Bhattacharya R, Cabral F (2004) A ubiquitous beta-tubulin disrupts microtubule assembly and inhibits cell proliferation. *Mol Biol Cell* 15:3123–3131. doi:10.1091/mbc.E04
- Bhattacharya R, Yang H, Cabral F (2011) Class V  $\beta$ -tubulin alters dynamic instability and stimulates microtubule detachment from centrosomes. *Mol Biol Cell* 22:1025–1034. doi:10.1091/mbc.E10-10-0822
- Bounoutas A, Hagan RO, Chalfie M (2009) The multipurpose 15-protofilament microtubules in *C. elegans* have specific roles in mechanosensation. *Curr Biol* 19:1362–1367. doi:10.1016/j.cub.2009.06.036
- Cloes M, Renson T, Johnen N et al (2013) Differentiation of Boettcher's cells during postnatal development of rat cochlea. *Cell Tissue Res* 354:707–716. doi:10.1007/s00441-013-1705-8
- Cowan NJ, Lewis SA, Gu W, Burgoyne RD (1988) Tubulin isotypes and their interaction with microtubule associated proteins. *Protoplasma* 145:106–111. doi:10.1007/BF01349346
- Etienne-Manneville S (2013) Microtubules in cell migration. *Annu Rev Cell Dev Biol* 29:471–499. doi:10.1146/annurev-cellbio-101011-155711
- Fritzsche B, Pan N, Jahan I, Elliott KL (2014) Inner ear development: building a spiral ganglion and an organ of Corti out of unspecified ectoderm. *Cell Tissue Res*. doi:10.1007/s00441-014-2031-5
- Fukushige T, Siddiqui ZK, Chou M et al (1999) MEC-12, an alpha-tubulin required for touch sensitivity in *C. elegans*. *J Cell Sci* 112(Pt 3):395–403
- Fulton C, Simpson PA (1976) Selective synthesis and utilization of flagellar tubulin. The multi-tubulin hypothesis. *Cell Motil* 3:987–1005
- Hallworth R, Ludueña RF (2000) Differential expression of beta tubulin isotypes in the adult gerbil cochlea. *Hear Res* 148:161–172. doi:10.1016/S0378-5955(00)00149-0
- Hallworth R, McCoy M, Polan-Curtain J (2000) Tubulin expression in the developing and adult gerbil organ of Corti. *Hear Res* 139:31–41. doi:10.1016/S0378-5955(99)00165-3
- Hari M, Wang Y, Veeraraghavan S, Cabral F (2003) Mutations in alpha- and beta-tubulin that stabilize microtubules and confer resistance to colcemid and vinblastine. *Mol Cancer Ther* 2:597–605
- Henderson CG, Tucker JB, Chaplin MA et al (1994) Reorganization of the centrosome and associated microtubules during the morphogenesis of a mouse cochlear epithelial cell. *J Cell Sci* 107(Pt 2):589–600
- Henderson CG, Tucker JB, Mogensen MM et al (1995) Three microtubule-organizing centres collaborate in a mouse cochlear epithelial cell during supracellularly coordinated control of microtubule positioning. *J Cell Sci* 108(Pt 1):37–50
- Jensen-Smith HC, Eley J, Steyger PS et al (2003) Cell type-specific reduction of  $\beta$  tubulin isotypes synthesized in the developing gerbil organ of Corti. *J Neurocytol* 32:185–197. doi:10.1023/B:NEUR.0000005602.18713.02
- Johnen N, Francart M-E, Thelen N et al (2012) Evidence for a partial epithelial-mesenchymal transition in postnatal stages of rat auditory organ morphogenesis. *Histochem Cell Biol* 138:477–488. doi:10.1007/s00418-012-0969-5
- Joshi HC, Chu D, Buxbaum RE, Heidemann SR (1985) Tension and compression in the cytoskeleton of PC 12 neurites. *J Cell Biol* 101:697–705. doi:10.1083/jcb.101.3.697
- Karavitiaki KD, Mountain DC (2007) Evidence for outer hair cell driven oscillatory fluid flow in the tunnel of Corti. *Biophys J* 92:3284–3293. doi:10.1529/biophysj.106.084087
- Lee HO, Norden C (2013) Mechanisms controlling arrangements and movements of nuclei in pseudostratified epithelia. *Trends Cell Biol* 23:141–150. doi:10.1016/j.tcb.2012.11.001
- Lewis SA, Lee MG, Cowan NJ (1985) Five mouse tubulin isotypes and their regulated expression during development. *J Cell Biol* 101:852–861. doi:10.1083/jcb.101.3.852
- Locher H, Frijns JHM, Huisman MA, de Sousa Lopes SMC (2013) TUBB3: neuronal marker or melanocyte mimic? *Cell Transplant*. doi:10.3727/096368913X674099
- Ludueña RF (1998) Multiple forms of tubulin: different gene products and covalent modifications. *Int Rev Cytol* 178:207–275. doi:10.1016/S0074-7696(08)62138-5
- Paras A, Webster P, Kalinec F (2012) Deiters cells tread a narrow path—the Deiters cells-basilar membrane junction. *Hear Res* 290:13–20. doi:10.1016/j.heares.2012.05.006
- Perry B, Jensen-Smith HC, Ludueña RF, Hallworth R (2003) Selective expression of beta tubulin isotypes in gerbil vestibular sensory epithelia and neurons. *J Assoc Res Otolaryngol* 4:329–338. doi:10.1007/s10162-002-2048-4

- Raff EC (1997) Microtubule architecture specified by a beta-tubulin isoform. *Science* 275:70–73. doi:[10.1126/science.275.5296.70](https://doi.org/10.1126/science.275.5296.70)
- Roach MC, Boucher VL, Walss C et al (1998) Preparation of a monoclonal antibody specific for the class I isotype of  $\beta$ -tubulin: the  $\beta$  isotypes of tubulin differ in their cellular distributions within human tissues. *Cell Motil Cytoskelet* 39:273–285. doi:[10.1002/\(SICI\)1097-0169\(1998\)39:4<273::AID-CM3>3.0.CO;2-4](https://doi.org/10.1002/(SICI)1097-0169(1998)39:4<273::AID-CM3>3.0.CO;2-4)
- Saillour Y, Broix L, Bruel-Jungerman E et al (2014) Beta tubulin isoforms are not interchangeable for rescuing impaired radial migration due to Tubb3 knockdown. *Hum Mol Genet* 23:1516–1526. doi:[10.1093/hmg/ddt538](https://doi.org/10.1093/hmg/ddt538)
- Savage C, Hamelin M, Culotti JG et al (1989) *mec-7* is a beta-tubulin gene required for the production of 15-prot filament microtubules in *Caenorhabditis elegans*. *Genes Dev* 3:870–881. doi:[10.1101/gad.3.6.870](https://doi.org/10.1101/gad.3.6.870)
- Slepecky NB, Henderson CG, Saha S (1995) Post-translational modifications of tubulin suggest that dynamic microtubules are present in sensory cells and stable microtubules are present in supporting cells of the mammalian cochlea. *Hear Res* 91:136–147. doi:[10.1016/0378-5955\(95\)00184-0](https://doi.org/10.1016/0378-5955(95)00184-0)
- Souter M, Nevill G, Forge A (1997) Postnatal maturation of the organ of Corti in gerbils: morphology and physiological responses. *J Comp Neurol* 386:635–651. doi:[10.1002/\(SICI\)1096-9861\(19971006\)386:4<635::AID-CNE9>3.0.CO;2-3](https://doi.org/10.1002/(SICI)1096-9861(19971006)386:4<635::AID-CNE9>3.0.CO;2-3)
- Steyger PS, Furness DN, Hackney CM, Richardson GP (1989) Tubulin and microtubules in cochlear hair cells: comparative immunocytochemistry and ultrastructure. *Hear Res* 42:1–16. doi:[10.1016/0378-5955\(89\)90113-5](https://doi.org/10.1016/0378-5955(89)90113-5)
- Szarama KB, Gavara N, Petralia RS et al (2012) Cytoskeletal changes in actin and microtubules underlie the developing surface mechanical properties of sensory and supporting cells in the mouse cochlea. *Development* (Cambridge, England) 139:2187–2197. doi:[10.1242/dev.073734](https://doi.org/10.1242/dev.073734)
- Tannenbaum J, Slepecky NB (1997) Localization of microtubules containing posttranslationally modified tubulin in cochlear epithelial cells during development. *Cell Motil Cytoskelet* 38:146–162. doi:[10.1002/\(SICI\)1097-0169\(1997\)38:2<146::AID-CM4>3.0.CO;2-5](https://doi.org/10.1002/(SICI)1097-0169(1997)38:2<146::AID-CM4>3.0.CO;2-5)
- Thelen N, Breuskin I, Malgrange B, Thiry M (2009) Early identification of inner pillar cells during rat cochlear development. *Cell Tissue Res* 337:1–14. doi:[10.1007/s00441-009-0810-1](https://doi.org/10.1007/s00441-009-0810-1)
- Tischfield MA, Baris HN, Wu C et al (2010) Human TUBB3 mutations perturb microtubule dynamics, kinesin interactions, and axon guidance. *Cell* 140:74–87. doi:[10.1016/j.cell.2009.12.011](https://doi.org/10.1016/j.cell.2009.12.011)
- Tucker JB, Paton CC, Richardson GP et al (1992) A cell surface-associated centrosomal layer of microtubule-organizing material in the inner pillar cell of the mouse cochlea. *J Cell Sci* 102(Pt 2):215–226
- Tucker JB, Mogensen MM, Henderson CG et al (1998) Nucleation and capture of large cell surface-associated microtubule arrays that are not located near centrosomes in certain cochlear epithelial cells. *J Anat* 192(Pt 1):119–130. doi:[10.1046/j.1469-7580.1998.19210119.x](https://doi.org/10.1046/j.1469-7580.1998.19210119.x)
- Wade RH (2009) On and around microtubules: an overview. *Mol Biotechnol* 43:177–191. doi:[10.1007/s12033-009-9193-5](https://doi.org/10.1007/s12033-009-9193-5)
- Yang H, Cabral F, Bhattacharya R (2009) Tubulin isotype specificity and identification of the epitope for antibody Tub 2.1. *Protein Eng Des Sel* 22:625–629. doi:[10.1093/protein/gzp046](https://doi.org/10.1093/protein/gzp046)
- Zagadou BF, Mountain DC (2012) Analysis of the cochlear amplifier fluid pump hypothesis. *J Assoc Res Otolaryngol* 13:185–197. doi:[10.1007/s10162-011-0308-x](https://doi.org/10.1007/s10162-011-0308-x)